DOI: 10.13009/EUCASS2023-799
Aerospace Europe Conference 2023 – 10TH EUCASS – 9TH CEAS

Diameter of Spherical Alumina Pt Catalyst: Influence on Hydrogen Peroxide Decomposition Performance & Catalytic Bed Ageing

*C. Cottenot**†§, *B. Boust**, *L. Prévost*†, *R. Beauchet*§, *Y. Batonneau*§ *and M. Bellenoue**

* *PPrime Institute, CNRS, ISAE-ENSMA, University of Poitiers, Chasseneuil-du-Poitou, France*
† *CNES, 52 rue Jacques Hillairet, 75612 Paris Cedex*
§ *IC2MP, CNRS-UMR 7285, Université de Poitiers, 4 rue Michel Brunet B27, TSA 51106, 86073, Poitiers Cedex 9, France*

camille.cottenot@ensma.fr, yann.batonneau@univ-poitiers.fr, marc.bellenoue@ensma.fr

Abstract

The use of different diameters of Pt/ Al_2O_3 spherical catalysts for HTP 98% decomposition (1 mm and 2 mm) enabled a better reactivity of the decomposition process for the smaller one, with quite comparable nominal performance and decomposition efficiency in ACSEL facility. In addition, a rapid physical degradation of the 1-mm catalyst proved harmful to the system, fines created during the damage caused partial clogging of the bed, resulting in a rise in the chamber pressure.

1. Introduction

In the current efforts to make space propulsion greener, low toxicity propellants such as High-Test Peroxide (HTP) are investigated to replace hydrazine, which could be banned by the European Registration, Evaluation, Authorization and Restriction of Chemicals (REACH) within a few years. Hydrogen peroxide can spontaneously decompose into gaseous dioxygen and water vapour through an exothermic disproportionation reaction enhanced by a catalytic reaction. This property is used in low-to-medium thrust propulsive applications for HTP at mass concentrations ranging from 70 to 99 %, allowing comparable performance to monopropellant hydrazine attitude control systems [1]. The high temperature dioxygen released subsequently to the decomposition can also be used towards fuel combustion for bipropellant applications [2]. In both situations, the quality and performance of decomposition, yielding a high temperature of the decomposed gases and a fast reactivity is essential. The choice of catalytic bed composition and loading thus plays a crucial part in the matter.

Noble metal particles [3] and manganese oxides [4] deposited onto ceramic materials [5] such as γ-phase alumina (γ-Al_2O_3) are commonly used as hydrogen peroxide catalysts. However, a great variety of different geometries [6] and dimensions of the selected support material have been studied, ranging from metal grids [7], to printed monoliths or pellets [8]. The chosen geometry [9] plays a key role in the decomposition performance [10]: smaller average dimensions of individual catalyst pellet for a given catalytic bed volume allow a higher surface area onto which deposited active phase is available for the decomposition of H_2O_2 molecules. This gain in performance is also expected to enable cold starts of the catalytic reaction, without any required preheating of the catalytic bed [11]. However, smaller dimensions of elementary catalyst support also induce less inter-granular porosity, causing more risks of pressure losses and clogging in the decomposed hydrogen peroxide flow within the catalyst bed. In this paper, two different diameters of spherical Pt-catalysts will be studied to investigate the differences in performance and longevity of the catalytic bed.

2. Catalysts

a. Preparation steps

Platinum was selected as an active phase due to its well-studied superior reactivity toward hydrogen peroxide decomposition [12], with a target weight ratio of 5 % in mass of both catalysts. Alumina spheres of 1 mm and 2 mm in diameter were chosen for the preparation of two different batches of catalysts. The spherical shape enables a constant particle aspect ratio of 1 and a theoretically optimal and stable packing efficiency. In total, the available surface accessible for hydrogen peroxide with the 1 mm diameter catalyst is doubled for a given catalyst bed volume, with respect to the 2 mm diameter catalyst.

DOI: 10.13009/EUCASS2023-799

Both raw alumina spheres first underwent a 2 h-long preheating treatment at 1283 K in a muffle furnace before impregnation. A stabilization of the specific surface area before the impregnation step was deemed necessary to avoid subjecting a non-treated, platinum-impregnated alumina to a high temperature calcination and reduction. This high temperature could cause a specific surface area drop due to a partial crystallization of the alumina, which could be detrimental to the dispersion of the deposited active phase. The impregnation step was then carried out on a more stabilized specific surface area alumina. A precursor solution of hexachloroplatinic acid was impregnated on the γ-Al_2O_3 spheres using the wet impregnation method. This step was followed by an overnight evaporation and drying. Finally, both impregnated alumina spheres of 1 mm and 2 mm underwent a calcination at 723 K under an O_2/Ar atmosphere, followed by a H_2/Ar reduction at 1283 K. The reduction temperature was selected to be 50 K above the adiabatic decomposition temperature of HTP 98 %. The two prepared catalysts will be further referenced as CC_1_1283 (1 mm diameter supporting material) and CC_2_1283 (2 mm diameter supporting material).

Fig. 1 presents a photograph of each prepared catalyst.

Fig. 1 Catalysts CC_1_1283 (left) and CC_2_1283 (right)

b. Chemical and physical analyses of catalysts

Catalysts were analysed using nitrogen sorptiometry (Tristar 2, Micromeritics) for measurement of the specific surface area using the BET method. Inductively-coupled plasma-optical emission spectrometry (ICP-OES, Agilent 5110) was used to determine the active phase mass fraction and hydrogen chemisorption (Micrometrics, Autochem 2920II) to calculate the dispersion in atomic percent of the active phase. The dispersion of the active phase is defined as the ratio of accessible platinum sites to the total amount of platinum deposited, and is inversely proportional to the average size of platinum nanoparticles deposited onto the catalyst support. The characterization results of the fresh catalysts are listed in Table 1, where the specific surface area of the catalysts is normalised by an arbitrary value.

Table 1 Properties of the two catalysts described above before tests.

	CC_1_1283	**CC_2_1283**
Supporting material diameter (mm)	1	2
Normalised specific surface area	0.92 ± 0.05	0.95 ± 0.05
Pt Dispersion (%)	79 ± 3	80 ± 3
Pt Mass fraction (%)	4.9 ± 0.1	4.8 ± 0.1

3. Experimental testing apparatus

a. ACSEL Facility and instrumentation

The catalysts were tested in the ACSEL facility, presented in Fig. 2. The bench is composed of a catalytic decomposition chamber allowing to assess the performance of HTP decomposition [13]. A mass of 20 g of the to-be-tested catalyst was put in the Catalytic Decomposition Chamber as shown in Fig. 2. The nominal Catalytic Bed Loading (CBL), as defined in Eq (1), is the ratio between the nominal mass flow rate of injected HTP $\dot{m}_{HTP}$ to the cross section of the catalyst bed A_{CDC}, was targeted at a value of 12 kg m^{-2} s^{-1}. The Catalyst Capacity (C_{cat}), defined in Eq (2) is the ratio of the mass flow rate of injected HTP $\dot{m}_{HTP}$ to the total volume of catalyst bed V_{CDC}, was targeted at a value of 0.3 g cm^{-3} s^{-1}. The facility is equipped with a 5 mm diameter exit throat. The oxidizer was injected through a 0.5 mm nozzle directly in the decomposition chamber at the nominal mass flow rate, controlled *via* a Coriolis mass flowmeter. The static pressure and temperature of the decomposed gases were recorded downstream of the catalytic chamber by a shielded K-thermocouple and a pressure sensor. A heating collar was placed around the catalytic chamber, in order to regulate and control the initial temperature of the catalyst between 300 K and 440 K *via* a K-thermocouple placed on the chamber wall.

DOI: 10.13009/EUCASS2023-799

$$CBL = \frac{\dot{m}_{HTP}}{A_{CDC}} \qquad \textit{Eq (1)}$$

$$C_{cat} = \frac{\dot{m}_{HTP}}{V_{CDC}} \qquad \textit{Eq (2)}$$

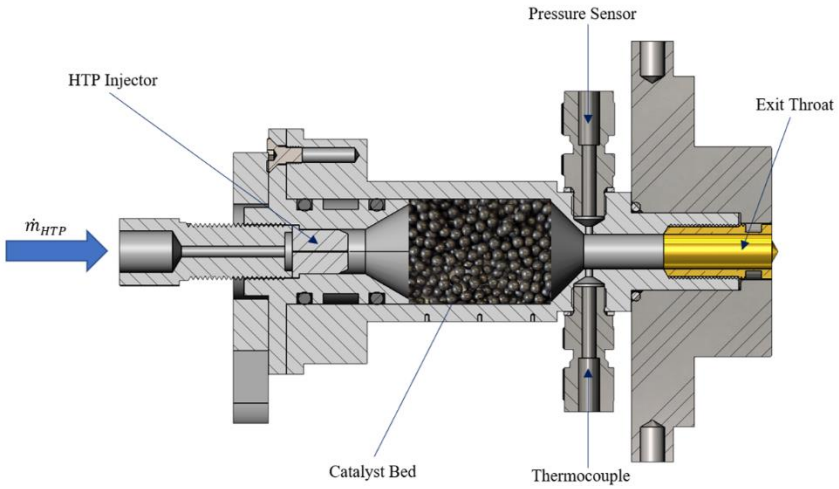

Fig. 2 Catalytic Decomposition Chamber of the ACSEL facility

Fig. 3 shows pressure, temperature and mass flow rate records obtained during a typical catalytic decomposition test. The recorded temperature of the decomposition gases downstream of the decomposition chamber is normalised by the adiabatic decomposition temperature of HTP 98 (1223 K). In total, roughly 90 g of HTP was injected and decomposed, in a test-sequence of 10 pulses of 500 ms each, followed by a plateau of 4 s for assessment of the nominal performance.

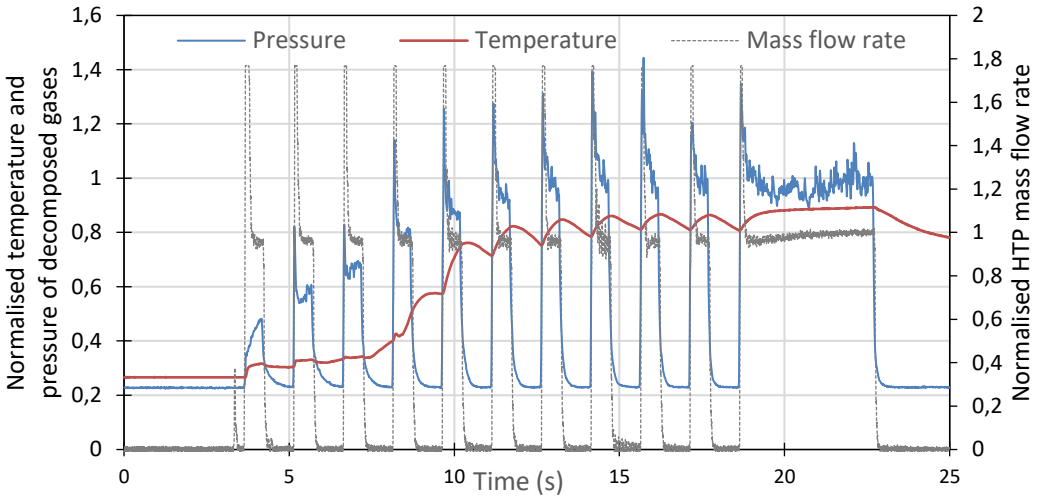

Fig. 3 Recorded data on a reference test carried out with CC_2_1283 catalyst for HTP 98% decomposition

The reference sequence carried out presented in Fig. 3 allowed to compare the rise in the temperature of the catalytically decomposed gases and pressure of the catalytic chamber, during several tests carried out for each of the two catalysts.

b. Hydrogen peroxide catalytic decomposition performance assessment

The characteristic velocity c^* of the hydrogen peroxide decomposition and its efficiency (η_{c^*}) are a crucial index of the decomposition performance. The measured characteristic velocity values $c^*_{measured}$ were evaluated for each test series from the average temperature recorded during the last second of the plateau, using Eq (3).

DOI: 10.13009/EUCASS2023-799

The characteristic velocity efficiency η_{c^*} is then evaluated by comparing $c^*_{measured}$ to the ideal value c^*_{ideal} as calculated in Eq (4). The value of the specific heat capacity γ_{adiab} and specific gas constant r_{adiab} of the assumed fully adiabatically decomposed hydrogen peroxide is determined numerically in a Cantera reactor of ideal gas using reduced kinetic scheme developed by Basevich et *al.* [15]. Similarly, the γ- and *r*–values in Eq (3) are calculated by the same means assuming a full decomposition of peroxide at the average recorded temperature (accounting for the heat losses within the catalytic bed). The total temperature T_{tot} is computed from the average recorded temperature of the decomposed gases downstream to the catalytic bed during the plateau, taking into account the flow Mach number computed at the measurement cross section.

$$c^*_{measured} = \sqrt{\frac{rT_{tot}}{\gamma}}\left(\frac{\gamma+1}{2}\right)^{\frac{\gamma+1}{2(\gamma-1)}}$$

Eq (3)

$$c^*_{ideal} = \sqrt{\frac{r_{adiab}T_{adiab}}{\gamma_{adiab}}}\left(\frac{\gamma_{adiab}+1}{2}\right)^{\frac{\gamma_{adiab}+1}{2(\gamma_{adiab}-1)}}$$

Eq (4)

$$\eta_{c^*} = \frac{c^*_{measured}}{c^*_{ideal}}$$

Eq (5)

The rising time of the decomposed gases temperature also allows assessment of the response time of the system. The rising time expressed in Eq (6) is defined as the time difference required for the catalyst bed temperature to increase from 5 % to 95 % of the average recorded temperature during the nominal plateau.

$$t_{rising} = t_{95\%} - t_{5\%}$$

Eq (6)

4. Results & discussions

a. Comparison of the decomposition performance

The difference in performance in terms of recorded temperature and pressure was first assessed at different initial temperatures of the catalytic bed: ambient room temperature, which can be considered a “cold start”, and ambient temperature + 100 K. The superimposition of the HTP 98% decomposed gases temperature response for each catalyst tested is presented in Fig. 4. Temperature is normalized using Eq (7), where T_{adiab} is the adiabatic decomposition temperature of HTP 98%, and T_{init} is the initial temperature of the catalytic bed.

$$\eta_T = \frac{T_{measured} - T_{init}}{T_{adiab} - T_{init}}$$

Eq (7)

First, both catalysts successfully activated the decomposition reaction at low initial temperature (cold start). For both initial catalytic bed temperatures, the catalyst CC_1_1283 showed a shorter rising time, that might result from a faster decomposition rate of HTP 98 %. Indeed, the smallest diameter catalyst, CC_1_1283, presents an increased overall surface area of accessible active phase for a given catalytic bed volume. The rising times, expressed in Eq (6), and hereby calculated by using η_T for the temperature values, are presented in Table 2. The values of rising times experimentally decrease with increasing initial temperature, as expected from the application of Arrhenius law.

Additionally, for both given initial temperatures, CC_1_1283 shows lower rising times compared to CC_2_1283. This can be interpreted as a faster reaction time regarding the decomposition reaction and rise in temperature.

DOI: 10.13009/EUCASS2023-799

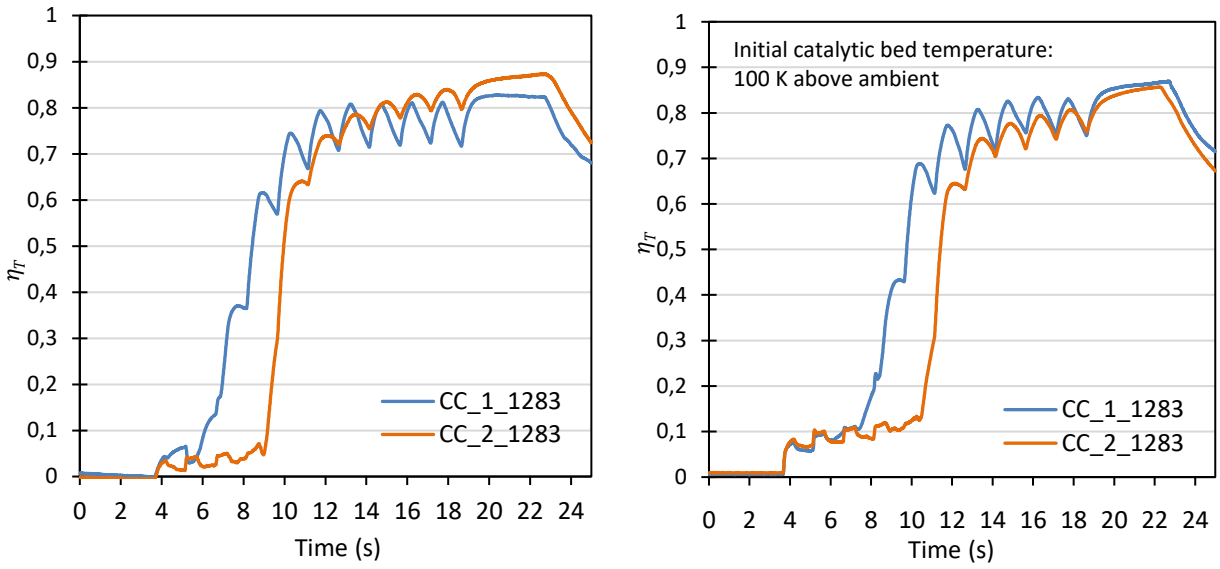

Fig. 4 Normalised temperature of the decomposed gases during an HTP 98% catalytic decomposition test sequence in the ACSEL facility, at ambient (left) and ambient+100 K initial catalytic bed temperatures (right)

Table 2 Rising times t_{rising} (in seconds) of decomposed gas temperature for each catalyst during a reference test sequence for HTP 98% decomposition tests at various initial catalytic bed preheating

t_{rising}/s	ambient	100 K above ambient
CC_1_1283	7.9	5.8
CC_2_1283	9.6	8.1

The comparison of the temperature rise was additionally accompanied by a study of the catalytic decomposition chamber pressure variations during the same carried-out tests. Fig. 5 presents the superimposition of the recorded pressure, normalized by the nominal pressure value record during the plateau, for the two catalysts during HTP 98% decomposition at the initial catalytic bed temperature of roughly 400 K. The pressure rises faster during decomposition with catalyst CC_1_1283. However, pressure peaks at the beginning of each pulse have been noted exclusively during the tests carried out with CC_1_1283. Major pressure oscillations such as those peaks may cause a catalytic bed clogging issue. This clogging might be provoked by an insufficient catalytic reactivity, leading to potential hydrogen peroxide accumulation. The built-up in undecomposed injected hydrogen peroxide causes peaks and a mechanical loading on the alumina, breaking the spheres and creating small fine particles in case of a lack of thermomechanical resistance. One can also note the faster draining of the pressure from the third pulse and between each pulse than in the case of CC_2_1283 catalyst, which is a direct consequence of the higher pressure during the pulses: a higher pressure difference between the catalytic decomposition chamber and the exhaust atmosphere implies a faster flushing of the gases.

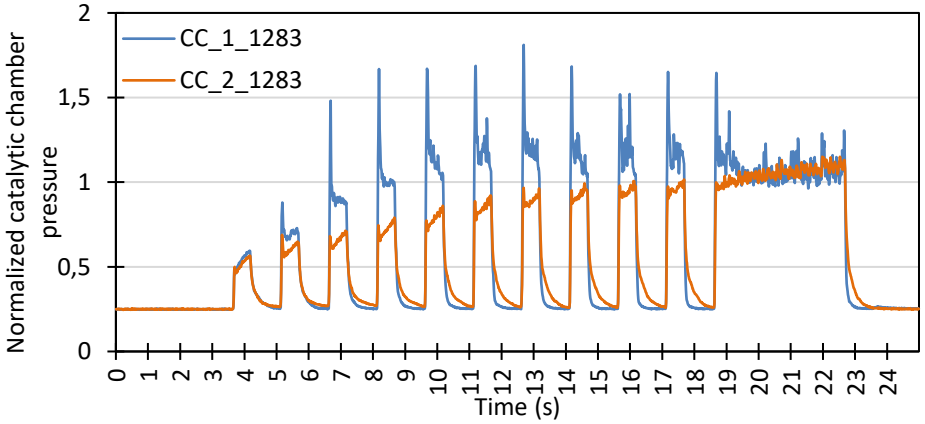

Fig. 5 Pressure of the catalytic decomposition chamber during an HTP 98% decomposition test sequence in the ACSEL facility, at an initial catalytic bed temperature of 393 K

DOI: 10.13009/EUCASS2023-799

The ageing of the catalysts is here defined as the quantity of HTP injected onto the catalyst (throughput), hence the mass of decomposed hydrogen peroxide (one can transpose this parameter as number of pulses as the test sequence has been kept constant during all series). The overall decomposition performance was computed and expressed in terms of characteristic velocity efficiency η_{c^*} during successive tests of the two catalysts. The evolution of the characteristic velocity efficiency thus obtained is shown in Fig. 6. One can notice the similar response in terms of characteristic velocity efficiency for both catalysts, in addition to an apparent stability of the performances from first to last tests, representing a cumulated peroxide throughput of *circa* 4 kg.

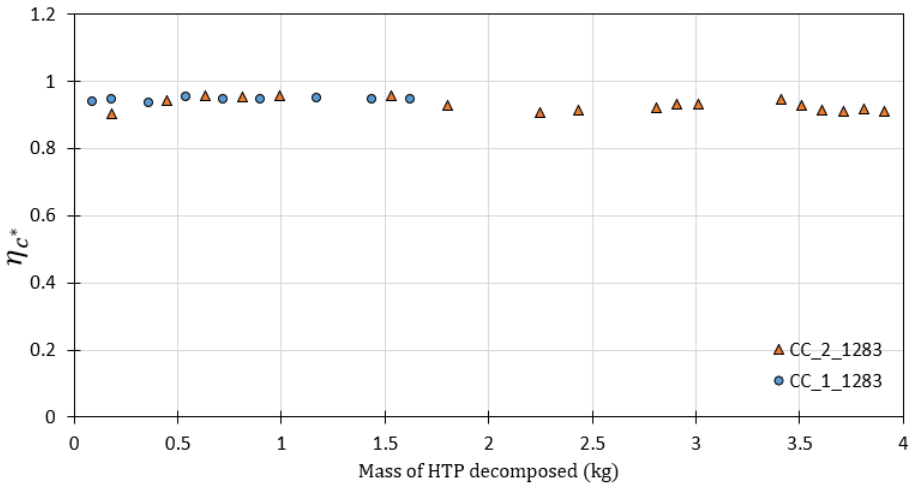

Fig. 6 Evolution of η_{c^*} with respect to HTP throughput

b. Catalysts evolution of physical properties throughout ageing.

The catalytic decomposition chamber was dismantled after each kilogram of ageing, which corresponds to approximately 10 to 12 tests, following the sequences shown in Fig. 7. After each dismantling of the set-up, 300 mg of catalyst was collected in the upstream part of the catalytic decomposition chamber. The sample was then analysed. The evolution of the specific surface area, normalised by an arbitrary value, and the platinum dispersion of the catalysts are presented in Fig. 7. Once analysed, the specimen was placed back in the ACSEL facility catalyst bed for further testing. A photograph of the dismantled upstream cross section ends of both catalytic beds prior to specimen collection after 1 kg of ageing is shown in Fig. 8.

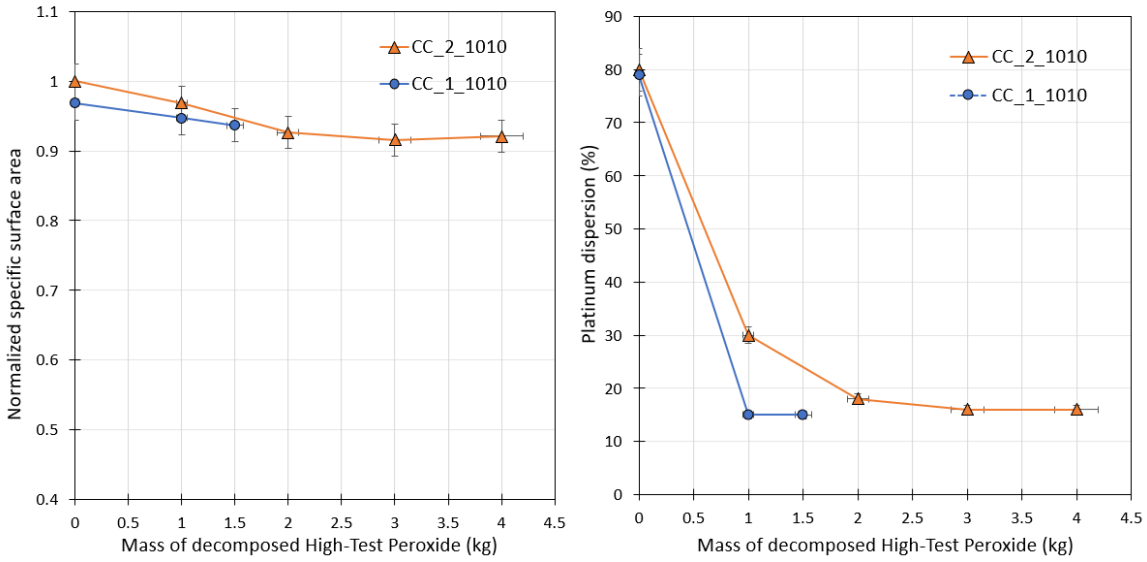

Fig. 7 Evolution of the catalysts specific surface area and platinum dispersion with their ageing

The specific surface area of both catalysts was weakly decreased after first tests, 2-mm spheres keeping their specific surface area stabilized above 90 % of its initial value. This accounts for quite an adequate temperature of thermal treatment during their preparation (1283 K). However, for both catalysts, the dispersion of the platinum significantly drops immediately after the first tests, even faster in the case of CC_1_1283 (1-mm diameter spheres).

DOI: 10.13009/EUCASS2023-799

Both platinum dispersion values seemingly appear to converge rapidly towards a value around 16%. Such a dispersion appears not to dramatically influence the performance of both catalytic beds as can be checked in Fig. 6.

Fig. 8 Visual inspection of the catalyst bed (inlet cross section) physical damage after decomposition 1 kg of HTP 98% for CC_1_1283 (left) and CC_2_1283 (right)

Catalyst CC_1_1283 presents important physical damage (cf Fig. 8Fig. 8), with clusters of agglomerated powdered debris of platinum impregnated alumina. Roughly 10 % of the catalytic mass was lost due to the created fines being ejected through the exit grid, compared to a 3 % mass loss for CC_2_1283. Due to too much physical breakage of the spheres, which raised concerns for the catalytic bed integrity regarding the pressure rise occurring during testing, CC_1_1283 tests were interrupted after 1.5 kg of HTP 98%. However, the platinum dispersion convergence trend still seems to be confirmed after 1.5 kg HTP. Additionally, the properties were first quantified after the decomposition of 1 kg HTP (10 tests sequences) but the downfall in the dispersion might have occurred as early as the first tests, which would have resulted in an even sleeper drop that is presented in Fig. 7.

5. Conclusion

The preparation and testing of two 5 % Pt/Al_2O_3 catalysts supported on alumina spheres of different diameters (1-mm and 2-mm spheres) allowed the study of the influence of said diameters on both performance of the catalytic reaction and some of their properties, as well as their evolution throughout their use. The rising times associated to the recorded temperature of the decomposition gases shows a faster response. This allows to conclude on the improved catalytic bed response and the need for a lesser amount of pulses to reach nominal values of temperature and pressure.

The performance in terms of characteristic velocity efficiency η_{c^*} remained quite similar, witnessing an unchanged overall efficiency of the catalytic decomposition during nominal use, whatever the sphere diameter or the propellant throughput. This particular observation can be partially explained by a low value of Catalyst Bed Loading (CBL) and Catalyst Capacity (C_{cat}) in the ACSEL facility: the section and length of the catalytic chamber, thus the volume of catalyst used, is important enough with respect to the injected HTP mas flow rate to compensate for any possible activity loss and performance. In the literature, CBL values for HTP monopropellant thrusters range from 5 kg m^{-2} s^{-1} [15] to more than 160 kg m^{-2} s^{-1} [10], and Catalyst Capacities from 0.16 g cm^{-3} s^{-1} [16] up to around 40 g cm^{-3} s^{-1} [17]. The ACSEL facility low range values of CBL (12 kg m^{-2} s^{-1}) and Catalyst Capacity (0.3 g cm^{-3} s^{-1}) shed a light on a both lower-than-average nominal mass flow rate and bigger-than-average catalytic bed volume.

However, the observed improvement of temperature rising with the use of a smaller diameter catalyst is yet counter-balanced by a much faster downfall of the catalyst platinum dispersion, as well as a partial clogging of the catalytic bed due to damage of the spheres and sintered non-evacuated fines. This prevented the catalytic bed of smaller size catalysts to be used for more than 15 tests, corresponding to roughly 1.5 kg of decomposed HTP 98%. Traditionally, to alleviate the pressure drop along the catalytic chamber bed, a bed composed of both smaller and bigger dimensions catalysts [16] [17] is implemented. The smaller diameter or dimensions catalysts are placed upstream of the catalytic bed, to enhance the performance and reactivity of the bed, and larger catalysts fill the rest of the downstream part of the bed, as a larger inter-granular porosity is more favourable to prevent clogging.

Acknowledgments

CNES is gratefully acknowledged for co-funding this study. This work was co-supported by the French government program "Investissements d'Avenir" (EUR INTREE, reference ANR-18-EURE-0010). Authors also acknowledge financial support from the European Union (ERDF) and "Région Nouvelle Aquitaine".

DOI: 10.13009/EUCASS2023-799

References

[1] Barley, S., Palmer, D., Wallbank, J. & Baker, D. (2005). Characterisation of a Monopropellant Microthruster Catalytic Bed. *41st AIAA/ASME/SAE/ASEE Joint Propulsion Conference & Exhibit*

[2] Okninski, A., Bartkowiak, B., Sobczak, K., Kublik, D., Surmacz, P., Rarata, G., Marciniak, B., & Wolanski, P. (2014). Development of a small green bipropellant rocket engine using hydrogen peroxide as oxidizer. *50th AIAA/ASME/SAE/ASEE Joint Propulsion Conference 2014*. https://doi.org/10.2514/6.2014-3592

[3] Pasini, A., Torre, L., Romeo, L., Cervone, A., & D'Agostino, L. (2008). Testing and characterization of a hydrogen peroxide monopropellant thruster. *Journal of Propulsion and Power*, *24*(3), 507–515. https://doi.org/10.2514/1.33121

[4] Surmacz, P., Rarata, G., Sobczak, K., Bartkowiak, B., Okninski, A., Wolanski, P., & Bel, F. V. (2017). Experimental evaluation of a catalyst bed based on MnxOy/Al2O3 catalyst for decomposition of 98% hydrogen peroxide. *53rd AIAA/SAE/ASEE Joint Propulsion Conference, 2017*. https://doi.org/10.2514/6.2017-4923

[5] Pirault-Roy, L., Kappenstein, C., Guérin, M., Eloirdi, R., & Pillet, N. (2002). Hydrogen peroxide decomposition on various supported catalysts effect of stabilizers. *Journal of Propulsion and Power*, *18*(6), 1235–1241. https://doi.org/10.2514/2.6058

[6] Reddy Nandyala, V., Batonneau, Y., Beauchet, R., Koopmans, R.-J., Nandyala, V., Pavesi, S., Ceribas, E., Maleix, C., Schwentenwein, M., Spitzbart, M., Altun, A., Mione, M., & Scharlemann, C. (2018). *Influence of Catalyst Geometry on Performance of Catalysts for Green Propellant Thrusters*. https://www.researchgate.net/publication/325284406

[7] Baumgartner, H. J., Hood, G. C., Monger, J. M., & Sanborn, C. E. (1963). Decomposition of Concentrated Hydrogen Peroxide on Silver II. High Temperature Decomposition. *Journal of Catalysis* (Vol. 2).

[8] An, S., Lee, J., Brahmi, R., Kappenstein, C., & Kwon, S. (2010). Comparison of catalyst support between monolith and pellet in hydrogen peroxide thrusters. *Journal of Propulsion and Power*, *26*(3), 439–445. https://doi.org/10.2514/1.46075

[9] Afandizadeh, S., & Foumeny, E. A. (n.d.). Design of packed bed reactors: guides to catalyst shape, size, and loading selection. *Applied Thermal Engineering 21 (2001) 669-682*. www.elsevier.com/locate/apthermeng

[10] Jo, S., Jang, D., An, S., & Kwon, S. (2011). Chugging instability of H2O2 monopropellant thrusters with catalyst reactivity and support sizes. *Journal of Propulsion and Power*, *27*(4), 920–924. https://doi.org/10.2514/1.B34222

[11] Jang, D., Kang, S., & Kwon, S. (2015). Preheating characteristics of H2O2 monopropellant thruster using manganese oxide catalyst. *Aerospace Science and Technology*, *41*, 24–27. https://doi.org/10.1016/j.ast.2014.12.010

[12] Dolci, S., Belli Dell'Amico, D., Pasini, A., Torre, L., Pace, G., & Valentini, D. (2015). Platinum catalysts development for 98% hydrogen peroxide decomposition in pulsed monopropellant thrusters. *Journal of Propulsion and Power*, *31*(4), 1204–1216. https://doi.org/10.2514/1.B35590

[13] Quintens, H., Boust, B., Bellenoue, M., Beauchet, R., & Batonneau, Y. (2022). *Experimental Comparison of Hydrogen Peroxide Catalysts for a Hydrogen Peroxide/n-Decane Bipropellant Combustor*. https://doi.org/10.2514/1.B38593

[14] Basevich, V. Y., Belyaev, A. A., Posvyanskii, V. S., & Frolov, S. M. (2013). Mechanisms of the oxidation and combustion of normal paraffin hydrocarbons: Transition from C1-C10 to C11-C16. *Russian Journal of Physical Chemistry B*, *7*(2), 161–169. https://doi.org/10.1134/S1990793113020103

[15] Ryan, C. N., Fonda-Marsland, E., Roberts, G. T., Lear, A., Fletcher, E., Giles, L., Palmer, M. J., & Gibbon, D. (2020). Experimental validation of a 1-newton hydrogen peroxide thruster. *Journal of Propulsion and Power*, *36*(2), 158–166. https://doi.org/10.2514/1.B37418

[16] Palmer, M. J., Musker, A. J., & Roberts, G. T. (2011). Experimental Assessment of Heterogeneous Catalysts for the Decomposition of Hydrogen Peroxide. *47th AIAA/ASME/SAE/ASEE Joint Propulsion Conference & Exhibit*

[17] Jung, S., Choi, S., Heo, S., & Kwon, S. (2021). Scaling of catalyst bed for hydrogen peroxide monopropellant thrusters using catalytic decomposition modeling. *Acta Astronautica*, *187*, 167–180. https://doi.org/10.1016/j.actaastro.2021.06.027

[18] Rang, S., An, S., Lim, H., & Kwon, S. (2006). Hydrogen Peroxide Gas Generator with Dual Catalytic Bed for Non-preheating Start-up. *47th AIAA/ASME/SAE/ASEE Joint Propulsion Conference & Exhibit*

[19] Heo, S., Jo, S., Yun, Y., & Kwon, S. (2018). Effect of dual-catalytic bed using two different catalyst sizes for hydrogen peroxide thruster. *Aerospace Science and Technology*, *78*, 26–32. https://doi.org/10.1016/j.ast.2018.03.032

DOI: 10.13009/EUCASS2023-799

[20] Romeo, L., Torre, L., Pasini, A., Cervone, A., SpA, A., & Calderazzo, F. (2007). Performance of Different Catalysts Supported on Alumina Spheres for Hydrogen Peroxide Decomposition. *43th AIAA/ASME/SAE/ASEE Joint Propulsion Conference & Exhibit*.

[21] Krejci, D., Schuh, S., Koopmans, R. J., & Scharlemann, C. (2015). Impact of catalyst length and preheating on transient catalytic 2O2 decomposition performance. *Journal of Propulsion and Power*, *31*(3), 985–988. https://doi.org/10.2514/1.B35489

[22] Pasini, A., Torre, L., Romeo, L., Cervone, A., & D'Agostino, L. (2008). Testing and characterization of a hydrogen peroxide monopropellant thruster. *Journal of Propulsion and Power*, *24*(3), 507–515. https://doi.org/10.2514/1.33121

[23] Jo, S. (2017). Response characteristics of H2O2 monopropellant thrusters with MnO2-mixed PbO catalyst. *Aerospace Science and Technology*, *60*, 1–8. https://doi.org/10.1016/j.ast.2016.10.022